Ann Thorac Cardiovasc Surg 2023; 29: 11–22
Online December 27, 2022
doi: 10.5761/atcs.oa.22-00090

Original Article

Circ_0006220 Contributes to NSCLC Progression through miR-342-3p/GOT2 Axis

Jichun Tang, Xuan Li, Lili Zhao, Jiajun Hui, and Ning Ding

Purpose: Dysregulated circular RNAs (circRNAs) have shown crucial modulatory functions in tumorigenesis, containing non-small cell lung cancer (NSCLC). The purpose of this study was to explore the biological functions and regulatory theory of circ_0006220 in NSCLC.
Methods: Reverse transcription-quantitative polymerase chain reaction and Western blot assay were conducted to measure RNA and protein expression, respectively. A total of 73 cases of NSCLC tumor samples were collected for expression analysis, and A-549 and NCI-H1299 cell lines were used for functional experiments. Cell proliferation was assessed by cell counting kit-8 assay, colony formation assay, 5-ethynyl-2'-deoxyuridine assay, and flow cytometry. Cell apoptosis, motility, and angiogenesis ability were analyzed by flow cytometry, transwell assays, and capillary-like network formation assay. Dual-luciferase reporter assay and RNA immunoprecipitation assay were conducted to verify the target relationships.
Results: Circ_0006220 was highly expressed in NSCLC tissues and cell lines. Circ_0006220 silencing inhibited the proliferation, migration, invasion, and angiogenesis but induced the apoptosis of NSCLC cells. Circ_0006220 acted as a microRNA-342-3p (miR-342-3p) sponge, and circ_0006220 knockdown-induced changes on the phenotypes of NSCLC cells were largely overturned by the knockdown of miR-342-3p. miR-342-3p interacted with the 3' untranslated region of glutamic-oxaloacetic transaminase 2 (GOT2), and GOT2 overexpression largely diminished miR-342-3p overexpression-mediated influences in NSCLC cells. Circ_0006220 could up-regulate GOT2 expression by sponging miR-342-3p.
Conclusion: Circ_0006220 promoted the malignant behaviors of NSCLC cells through mediating the miR-342-3p/GOT2 regulation cascade.

Keywords: non-small cell lung cancer, circ_0006220, miR-342-3p, GOT2

Department of Medical of Oncology, Wuxi Huishan District People's Hospital, Wuxi, Jiangsu, China

Received: May 25, 2022; Accepted: October 10, 2022
Corresponding author: Ning Ding. Department of Medical of Oncology, Wuxi Huishan District People's Hospital, No. 2, North Zhanqian Road, Luoshe Town, Huishan District, Wuxi, Jiangsu 214187, China
Email: ningmoli12@126.com

Introduction

Lung cancer is a high-risk malignancy.[1] According to the differences in pathological and etiological aspects, there are two subtypes of lung cancer, including non-small cell lung cancer (NSCLC) and small cell lung cancer (SCLC).[2] With the proportion of about 80%, NSCLC is the major subtype of lung cancer.[3] Although a significant progression has been made in the prevention, diagnosis, and treatment, the 5-year survival rate of NSCLC patients is still far from satisfactory.[2,4] Therefore, identifying novel effective molecular targets is essential in NSCLC treatment.

Circular RNAs (circRNAs) are a special class of non-coding RNAs with covalently closed continuous loop structure via back-splicing.[5] CircRNAs are more stable than linear RNAs because of their closed loop structure and are ideal biomarkers for human diseases. CircRNAs can bind to RNA-binding proteins to regulate the expression of target genes.[6] In addition, circRNAs are also known as miRNA sponges, which interact with miRNAs through miRNA response elements (MREs) to release messenger RNAs (mRNAs) from the inhibition of miRNAs, thereby resulting in the upregulation of downstream mRNAs.[7,8] CircRNAs are widely dysregulated in human cancers, and many researchers have revealed the pivotal regulatory roles of circRNAs in tumorigenesis, including NSCLC.[9–11] For instance, circ_0000376 is reported to contribute to cell proliferation, motility, and drug-resistance in NSCLC cells.[12] Circ_0006220 is a functional circRNA derived from transcriptional adaptor 2A (TADA2A) that is suggested to have elevated expression in NSCLC tissues via analyzing the GSE101586 data from Gene Expression Omnibus (GEO) public database. However, the biological significance behind the abnormal upregulation of circ_0006220 in NSCLC remains unclear.

Through StarBase database, we found that miR-342-3p harbored the seed sequence with circ_0006220. Previous studies demonstrated that miR-342-3p restrains the malignant behaviors of NSCLC cells by regulating LIM And SH3 Protein 1 (LASP1)[13], Ras-related protein Rap-2b (RAP2B),[14] or Anterior gradient protein 2 homolog (AGR2).[15] In this study, we analyzed the interaction and functional correlation between circ_0006220 and miR-342-3p in NSCLC cells.

Glutamic-oxaloacetic transaminase 2 (GOT2) is an aspartate aminotransferase, and it is implicated in the metabolic process of cancer cells in multiple aspects.[16–18] Jin *et al*. found that circ-SEC31A aggravates NSCLC development by binding to miR-520a-5p to increase GOT2 expression.[19] StarBase database predicted that GOT2 possessed the complementary sites with miR-342-3p. In this study, the binding relationship and functional relevance between miR-342-3p and GOT2 were explored in NSCLC.

The expression pattern and structural feature of circ_0006220 were first analyzed. Through knockdown experiments, we assessed the roles of circ_0006220 in regulating the phenotypes of NSCLC cells. Finally, the downstream signaling of circ_0006220 was explored by bioinformatics database and verified by rescue experiments.

Materials and Methods

Tissue specimens

NSCLC tissue specimens and corresponding healthy lung specimens were harvested after acquiring the written informed consents from 73 patients at Wuxi Huishan District People's Hospital. Serum samples from NSCLC patients (n = 32) and healthy volunteers (n = 20) were collected at Wuxi Huishan District People's Hospital. Patients receiving either chemotherapy or radiotherapy were excluded in this clinical experiment. Tissue specimens were stored at −80°C before RNA isolation. Human materials were utilized with the authorization of the Ethics Committee of Wuxi Huishan District People's Hospital (Approval No. 20210428).

Cell lines and cultivation

Normal lung cell line BEAS-2B, two common NSCLC cell lines (A-549 and NCI-H1299), and human umbilical vein endothelial cell line (HUVEC) were acquired from BeNa Culture Collection (Beijing, China) and cultivated in a complete medium at 37°C and 5% CO_2 atmosphere, which contained Dulbecco's Modified Eagle Medium (DMEM; Gibco, Carlsbad, CA, USA), 10% fetal bovine serum (FBS; Thermo Fisher Scientific, Waltham, MA, USA), and 1% antibiotic mixture (Gibco).

Subcellular fractionation

The distribution ratio of circ_0006220 in cell nuclear fraction and cytoplasmic fraction was evaluated via the commercial PARIS™ Kit Protein and RNA Isolation System (Thermo Fisher Scientific).

RNase R digestion

RNase R (3 U/μg; Epicentre Technologies, Madison, WI, USA) was added to RNA samples for 40 min. Subsequently, RNA expression was determined by reverse transcription-quantitative polymerase chain reaction (RT-qPCR).

RT-qPCR

For miR-342-3p, RNA was reverse-transcribed using miRNA-specific primer (Ribobio, Guangzhou, China). For circ_0006220, TADA2A, and GOT2, complementary DNA (cDNA) was synthesized using commercial Bio-Rad iScript kit (Bio-Rad, Hercules, CA, USA). qPCR reaction was implemented via commercial iQ SYBR Green Supermix reagents (Bio-Rad) and primers (**Supplementary Table 1**; all supplementary files are available online). The relative abundance of molecules

was analyzed as 2 (-Delta Delta C(T))[20] and normalized to the references.

Cell transfection

The specific small interference (si)RNAs targeting the back-splicing sites of circ_0006220 (si-circ_0006220#1, #2, and #3), negative control siRNA (si-NC), circ_0006220 overexpression plasmid (circ_0006220), circRNA NC vector pLO-ciR (circ-NC), miR-342-3p, NC, anti-miR-342-3p, anti-NC, GOT2 re-constructed plasmid (GOT2), and pcDNA plasmid (vector) were provided by GenePharma (Shanghai, China) and Ribobio.

Short hairpin (sh)RNA targeting circ_0006220 was designed and subcloned into a lentiviral vector pGLV2-U6-Puro (GenePharma) to form a Lenti-sh-circ_0006220 construct. The Lenti-sh-circ_0006220 or negative control lentiviral (Lenti-sh-NC) was packaged and harvested from 293T cells. The supernatant of 293T cells was collected and then infected A-549 cells for 5 h with polybrene. Stable cell lines were selected using puromycin (5.0 μg/ml for 5 days). The knockdown of circ_0006220 was evaluated by qRT-PCR.

Cell Counting Kit-8 (CCK8) assay

NSCLC cells were plated onto 96-well plates, and cell viability was examined via the commercial CCK8 kit (Beyotime, Jiangsu, China) after transfecting for the indicated time points. The optical density was examined at 450 nm.

Colony formation assay

Transfected NSCLC cells were harvested and re-suspended in a medium to obtain low-density cell suspension. Cell suspension was pipetted into 6-well plates. NSCLC cells were continued to culture for 14 days in a DMEM medium added with 10% FBS. Colonies were photographed and counted after they were immobilized and stained.

5-Ethynyl-2'-deoxyuridine (EdU) assay

Commercial EdU Cell Proliferation Kit (Ribobio) was adopted in this assay. NSCLC cells were cultured in the EdU-mixed medium for 2 h. Hoechst 33342 reagent (Sigma, St. Louis, MO, USA) was used to mark cell nucleus. Cells were imaged via the fluorescence microscope (Olympus, Tokyo, Japan).

Flow cytometry (cell cycle)

After fixing, NSCLC cells were re-suspended, and RNA content was digested through incubating with 10 μM RNase (Sangon Biotech, Shanghai, China) at 37°C for 30 min. DNA content was marked through staining with propidium iodide (PI; Sigma) at 4°C for 1 h. The ratio of NSCLC cells at different phases of cell cycle progression was evaluated on the FACS Calibur flow cytometer (BD Biosciences, Franklin Lakes, NJ, USA).

Flow cytometry (cell apoptosis)

Transfected NSCLC cells were first suspended in Annexin-V binding buffer (BestBio, Shanghai, China), and then the phosphatidylserine and DNA content were marked with Annexin V-fluorescein isothiocyanate (FITC) and PI of Annexin V-FITC/PI Detection Kit (BestBio). The apoptotic NSCLC cells with $FITC^+$ and $PI^{+/-}$ were distinguished from necrotic cells and normal cells via a FACSCalibur flow cytometer (BD Biosciences).

Transwell assays

Cell migration and invasion abilities were analyzed using cell culture inserts (8.0 μm pore; Costar, Corning, NY, USA). Transfected NSCLC cells were serum-starved for 24 h and then plated onto the compartments that coated with (to assess cell invasion capacity) or without (to assess cell migration capacity) Matrigel (BD Biosciences) in a serum-free medium. The lower chambers were filled with culture medium plus 10% FBS. Cells that migrated or invaded through the membrane were fixed, stained, and photographed at 100×.

Capillary-like network formation assay

The culture supernatant of transfected NSCLC cells was added to the wells of 96-well plates that coated with Matrigel (BD Biosciences) and plated with HUVECs. Cells were cultured at 37°C and 5% CO_2 for 10 h. Cell angiogenesis capacity was evaluated through counting the number of tubes in each node in random visual fields.

Western blot assay

Radioimmunoprecipitation assay lysis buffer (Sigma) was adopted to obtain protein samples. Forty micrograms of protein samples were run on sodium dodecyl sulfate-polyacrylamide gel electrophoresis and blotted onto the polyvinylidene fluoride membrane (Millipore, Billerica, MA, USA). After sealing for 1 h in 5% milk, primary antibodies were incubated with the membrane, including anti-Cyclin D1 (ab40754; Abcam, Cambridge, MA, USA), anti-caspase 3 (ab13585; Abcam), anti-matrix metallopeptidase 2 (anti-MMP2; ab181286; Abcam), anti-matrix metallopeptidase 2 (anti-MMP9; ab137867; Abcam),

anti-GOT2 (SAB2100950; Sigma), anti-proliferating cell nuclear antigen (anti-PCNA; ab29; Abcam), and anti-β-Actin (ab8226; Abcam). After washing using Tris buffered saline–Tween 20 (Sangon Biotech) for 3 times, secondary antibody (Abcam) was added to mark the primary antibodies. Protein bands were determined using chemiluminescence reagents (Bio-Rad).

Bioinformatics database

The GSE101586 dataset,[21] which was downloaded from the GEO datasets, analyzed circRNA expression profile in five pairs of lung adenocarcinoma tissues and adjacent healthy tissues by microarrays.

CircRNA–miRNA interactions and miRNA–mRNA interactions were predicted using StarBase database (http://starbase.sysu.edu.cn).

Dual-luciferase reporter assay

Full length fragment of circ_0006220 and the 3' untranslated region (3' UTR) of GOT2 as well as their corresponding mutant sequences were cloned into pmirGLO vector (Promega, Madison, WI, USA). These constructed plasmids were termed as circ_0006220-wt, circ_0006220-mut, GOT2-wt, and GOT2-mut. NC or miR-342-3p was co-transfected into NSCLC cells with luciferase plasmids. Luciferase intensities were determined using the dual-luciferase detection kits (Promega). Renilla luciferase activity was regarded as the control.

RNA immunoprecipitation (RIP) assay

The magnetic beads of EZ-Magna RIP™ RNA-Binding Protein Immunoprecipitation Kit (Millipore) were incubated with antibody against Argonaute2 (Millipore) or immunoglobulin G (Millipore) to obtain antibody-coated beads. NSCLC cells were lysed using lysis buffer added with RNase inhibitor (Millipore), and RNA samples were incubated with antibody-coated beads. The enriched RNAs were examined by RT-qPCR.

Xenograft tumors in nude mice

A total of ten nude mice (strain: BALB/c) from Vital River Laboratory Animal Technology (Beijing, China) were split into two groups (n = 5). Cell suspension was prepared using A-549 cells (3×10^6) stably expressing Lenti-sh-NC or Lenti-sh-circ_0006220. Cell suspension was then subcutaneously inoculated into the nude mice. The length and width of the xenograft tumors were measured using a vernier caliper every 5 days, and tumor size was assessed as length × width^2 × 0.5. Nude mice were killed via CO_2 asphyxia method after 30-d inoculation, and tumors were resected and weighed. RT-qPCR and Western blot assay were utilized to analyze RNA and protein expression. Immunohistochemistry (IHC) assay was implemented to detect ki-67 abundance using its antibody (ab833; Abcam) at the dilution of 1:100. This assay had gotten the authorization of the Animal Research Committee of Wuxi Huishan District People's Hospital.

Statistical analysis

Through GraphPad Prism 7.0 software (GraphPad, La Jolla, CA, USA), the results were analyzed and expressed as mean ± standard deviation (SD). The survival curve of patients was drawn by Kaplan–Meier plot and evaluated by the log-rank test. Linear correlation was analyzed by Pearson correlation coefficient. The data were analyzed by Student's *t*-test or one-way analysis of variance. Values of $P < 0.05$ were considered to be indicative of statistical significance.

Results

Circ_0006220 expression is elevated in NSCLC tissues and cell lines

The data of GSE101586 dataset revealed that circ_0006220 was upregulated in five NSCLC tumor specimens relative to that in adjacent normal lung tissues (**Fig. 1A**). Circ_0006220 is a circular transcript derived from the back-splicing of its host gene TADA2A. To confirm the expression pattern of circ_0006220 in NSCLC, we collected 73 pairs of NSCLC tissues and adjacent normal tissues. Compared with adjacent normal tissues (n = 73), circ_0006220 expression was observed to be markedly elevated in NSCLC tissues (n = 73) (**Fig. 1B**). Next, we measured the expression of circ_0006220 in the serum samples of NSCLC patients (n = 32) and healthy volunteers (n = 20). We found that circ_0006220 was markedly upregulated in the serum samples of NSCLC patients (**Supplementary Fig. 1**), suggesting that it might be a novel biomarker for the diagnosis of NSCLC. Next, patients were grouped as a high circ_0006220 group and a low circ_0006220 group based on the median level of circ_0006220. It was found that higher circ_0006220 expression was correlated with advanced TNM (primary tumor [T], regional lymph nodes [N], and distant metastases [M]) stages and distant metastasis (**Supplementary Table 2**). Also, circ_0006220 was upregulated in NSCLC cell lines including A-549 and NCI-H1299 compared

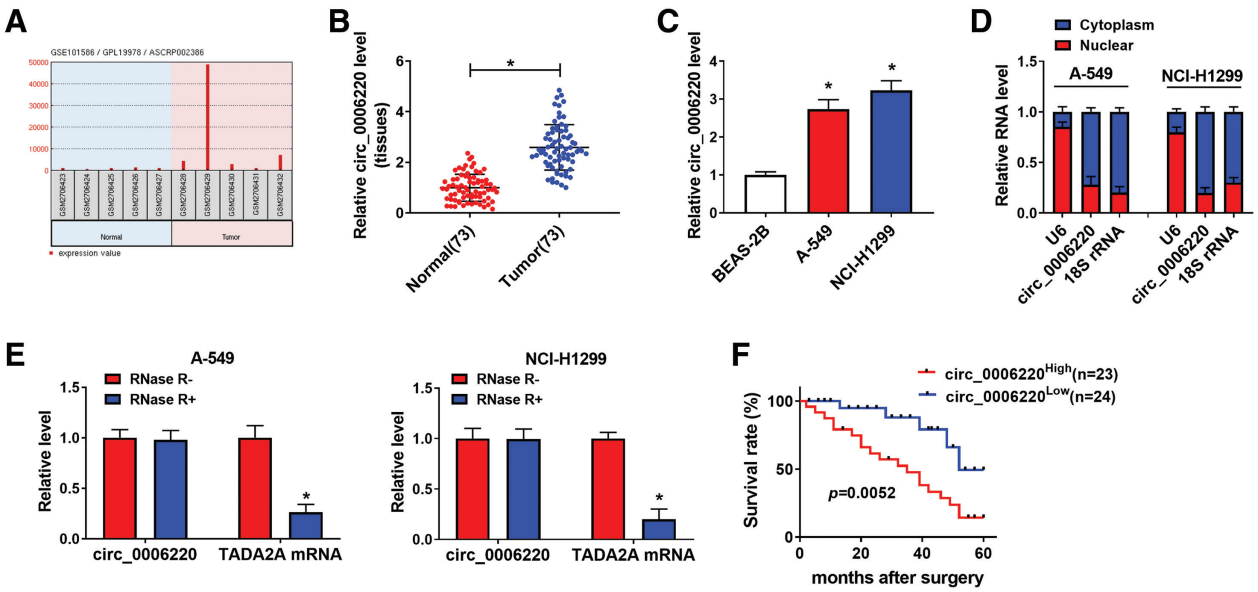

Fig. 1 Circ_0006220 expression is elevated in NSCLC tissues and cell lines. (**A**) Based on the data of GSE101586 dataset, the expression of circ_0006220 in five pairs of NSCLC tissues and adjacent normal tissues was shown. (**B**) RT-qPCR was adopted to measure the expression of circ_0006220 in 73 pairs of NSCLC tissues and matched normal tissues. (**C**) The level of circ_0006220 in two NSCLC cell lines including A-549 and NCI-H1299 along with BEAS-2B cell line was examined by RT-qPCR. (**D**) The subcellular localization of circ_0006220 was analyzed with U6 and 18S rRNA as references. (**E**) Exonuclease RNase R was used to analyze whether circ_0006220 was a circular transcript with its linear form TADA2A as reference. (**F**) NSCLC patients were divided into circ_0006220^{high} group and circ_0006220^{low} group with the median value of circ_0006220 expression as the cutoff. The 5-year survival rate curve of NSCLC patients in two groups was drawn. **P* <0.05. NSCLC: non-small cell lung cancer; RT-qPCR: reverse transcription-quantitative polymerase chain reaction; TADA2A: transcriptional adaptor 2A

with BEAS-2B cell line (**Fig. 1C**). With U6 and 18S rRNA as nuclear marker and cytoplasmic marker, we found that circ_0006220 was majorly localized in the cytoplasm of NSCLC cells (**Fig. 1D**), manifesting the potential of circ_0006220 to be a miRNA sponge. Exonuclease RNase R can only digest linear RNA with 3' terminal but not circRNAs. Thus, we tested whether circ_0006220 was a circular transcript using RNase R. As shown in **Fig. 1E**, RNase R addition markedly degraded linear TADA2A mRNA but not circ_0006220, suggesting that circ_0006220 was indeed a circular transcript. To analyze the association between circ_0006220 expression and the prognosis of NSCLC patients, NSCLC patients (n = 47) were followed up for 5 years to draw a survival curve. NSCLC patients were divided into two groups with the median value of circ_0006220 expression as the cutoff. Patient death was recorded as 1, and patient survival or loss to follow-up (for whatever reason) was recorded as 0. The results showed that patients with high circ_0006220 expression had shorter survival time than those with low circ_0006220 expression based on Kaplan–Meier survival curve analysis (**Fig. 1F**). Overall, circ_0006220 might regulate NSCLC progression.

Circ_0006220 exerts an oncogenic role in NSCLC cells

To clarify the role of circ_0006220 in NSCLC cells, we designed three circ_0006220-specific siRNAs, named as si-circ_0006220#1, si-circ_0006220#2, and si-circ_0006220#3. As verified by RT-qPCR, circ_0006220 expression was markedly reduced in three knockdown groups, with the highest knockdown efficiencies in si-circ_0006220#1 and si-circ_0006220#2 groups (**Fig. 2A**). CCK8 assay uncovered that circ_0006220 knockdown restrained the proliferation of NSCLC cells (**Fig. 2B**). Circ_0006220 silencing caused a notable reduction in the colony number than that in the si-NC group (**Fig. 2C**). The percentage of EdU$^+$ cells was reduced by circ_0006220 silencing (**Fig. 2D**). The fraction of NSCLC cells in the S phase was reduced by circ_0006220 knockdown, whereas the fraction of cells in the G0/G1 phase was elevated (**Fig. 2E**), indicating that circ_0006220 silencing induced cell cycle arrest in G1/S transition. The apoptotic rate of both NSCLC cell lines was markedly increased by circ_0006220 silencing (**Fig. 2F**). The silence of circ_0006220 decreased the numbers of migratory and invasive cells (**Figs. 2G** and

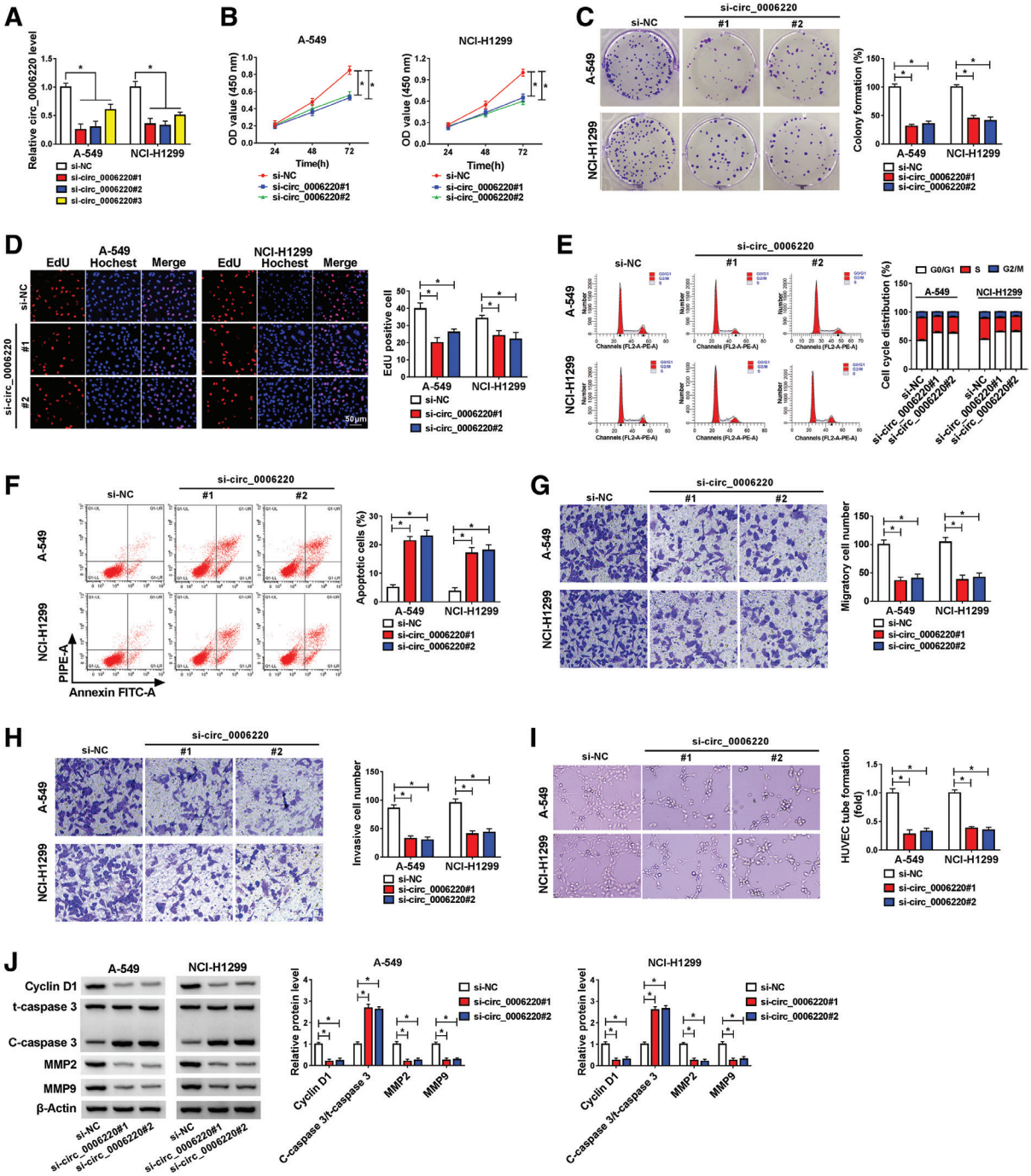

Fig. 2 Circ_0006220 exerts an oncogenic role in NSCLC cells. (**A**) The knockdown efficiencies of circ_0006220-specific siRNAs (si-circ_0006220#1, si-circ_0006220#2 and si-circ_0006220#3) were determined by RT-qPCR. (**B**–**J**) NSCLC cells were introduced with si-NC, si-circ_0006220#1, or si-circ_0006220#2. (**B**) CCK8 assay was conducted to draw cell proliferation curve. (**C**) Colony formation assay was performed to assess cell proliferation ability. (**D**) EdU assay was used to analyze the rate of DNA synthesis through measuring the incorporating of EdU. (**E**) Cell cycle distribution (G0/G1, S, and G2/M) was analyzed by flow cytometry. (**F**) Flow cytometry was applied to measure the apoptotic rate of NSCLC cells. (**G** and **H**) Transwell assays were adopted to analyze cell migration and invasion abilities. (**I**) Capillary-like network formation assay was adopted to show the formation of capillary-like structures. (**J**) Western blot assay was performed to measure the protein expression of proliferation marker (Cyclin D1), apoptosis marker (caspase 3), and motility marker (MMP2 and MMP9). *P <0.05. NSCLC: non-small cell lung cancer; RT-qPCR: reverse transcription-quantitative polymerase chain reaction; si-NC: negative control siRNA; CCK8: Cell Counting Kit-8; EdU: 5-ethynyl-2'-deoxyuridine; PIPE-A: propidium iodide/phycoerythrin-Area under curve; MMP2: matrix metallopeptidase 2; MMP9: matrix metallopeptidase 9; FITC: fluorescein isothiocyanate; HUVEC: human umbilical vein endothelial cell line

2H), manifesting that circ_0006220 knockdown blocked the migration and invasion of NSCLC cells. Circ_0006220 silencing suppressed the tube formation ability of NSCLC cells (**Fig. 2I**). Circ_0006220 interference reduced the expression of Cyclin D1, MMP2, and MMP9 but upregulated the level of cleaved caspase 3 (C-caspase 3)/total caspase 3 (t-caspase 3) (**Fig. 2J**), indicating that circ_0006220 knockdown suppressed cell proliferation and motility but induced cell apoptosis in NSCLC cells. Overall, circ_0006220 knockdown suppressed NSCLC progression *in vitro*.

Circ_0006220 acts as a sponge for miR-342-3p

CircRNAs are reported to mediate post-transcriptional regulation of genes by interacting with miRNAs.[22] By searching StarBase database, we predicted the possible miRNA targets of circ_0006220. A total of eight miRNAs (miR-221-3p, miR-222-3p, miR-483-3p, miR-342-3p, miR-520f-3p, miR-214-3p, miR-761, and miR-3619-5p) were predicted to be potential targets of circ_0006220. We analyzed the regulatory relationships between circ_0006220 and these miRNAs, and found that miR-342-3p was significantly negatively regulated by circ_0006220 in H1299 cells. Therefore, we further explored the binding relationship between circ_0006220 and miR-342-3p. The putative binding sites between circ_0006220 and miR-342-3p are shown in **Fig. 3A**. To verify that, dual-luciferase reporter assay and RIP assay were conducted. With the overexpression of miR-342-3p, the luciferase activity of wild-type reporter plasmid (circ_0006220-wt) but not mutant plasmid (circ_0006220-mut) was notably decreased (**Fig. 3B**). RIP assay further validated the binding between circ_0006220 and miR-342-3p because of the simultaneous enrichment of circ_0006220 and miR-342-3p in RNA-induced silencing complex (**Fig. 3C**). The transfection efficiency of circ_0006220 plasmid in NSCLC cells was confirmed (**Fig. 3D**). Circ_0006220 overexpression reduced miR-342-3p level, and miR-342-3p expression was markedly elevated in circ_0006220-silenced NSCLC cells (**Fig. 3E**). miR-342-3p was significantly downregulated in NSCLC tumor tissues than that in adjacent normal tissues (**Fig. 3F**). An inverse correlation between the expression of circ_0006220 and miR-342-3p was observed (**Fig. 3G**). Compared with BEAS-2B cell line, miR-342-3p expression was reduced in both NSCLC cell lines (**Fig. 3H**). Overall, circ_0006220 directly interacted with miR-342-3p in NSCLC cells.

Circ_0006220 plays an oncogenic role partly by sponging miR-342-3p in NSCLC cells

Transfection efficiency of anti-miR-342-3p was confirmed in NSCLC cells (**Fig. 4A**). To investigate whether circ_0006220 functioned by targeting miR-342-3p, compensation experiments were performed. Circ_0006220 silencing-induced upregulation of miR-342-3p was diminished by the addition of anti-miR-342-3p (**Fig. 4B**). As verified by CCK8 assay (**Fig. 4C**), colony formation assay (**Fig. 4D**), EdU assay (**Fig. 4E**), and flow cytometry (**Fig. 4F**), we found that circ_0006220 silencing-induced suppressive effect on cell proliferation of NSCLC cells was largely attenuated by the knockdown of miR-342-3p. Cell apoptosis was triggered by circ_0006220 silencing, and the introduction of anti-miR-342-3p largely reduced the apoptotic rate (**Fig. 4G**). The addition of anti-miR-342-3p also largely rescued the migration and invasion abilities of circ_0006220-silenced NSCLC cells, as verified by the increased numbers of migratory and invasive cells in si-circ_0006220#1 and anti-miR-342-3p co-transfected groups (**Figs. 4H** and **4I**). Cell angiogenesis ability was also largely recovered by the addition of anti-miR-342-3p (**Fig. 4J**). The introduction of anti-miR-342-3p largely recovered the expression of Cyclin D1, MMP2, and MMP9 and reduced the level of C-caspase 3/t-caspase 3 (**Fig. 4K**). Overall, circ_0006220 silencing-mediated antitumor effects were partly dependent on the upregulation of miR-342-3p.

GOT2 is controlled by circ_0006220/miR-342-3p axis, and circ_0006220 exerts its oncogenic roles via miR-342-3p/GOT2 axis

To further disclose the molecular mechanism of miR-342-3p in regulating NSCLC progression, the downstream targets of miR-342-3p were sought by StarBase database. We examined GOT2, which harbored the potential binding sequence with miR-342-3p at its 3' UTR (**Fig. 5A**). Next, we conducted dual-luciferase reporter assay and RIP assay to test their binding relation. As shown in **Fig. 5B**, the wild-type plasmid (GOT2-wt) exhibited lower luciferase activity in NSCLC cells expressing miR-342-3p than that in cells expressing scramble control. However, luciferase activity of mutant plasmid (GOT2-mut) was unaffected in cells expressing miR-342-3p or scramble control (**Fig. 5B**), suggesting the target relation between miR-342-3p and GOT2. RIP assay further verified the binding between miR-342-3p and GOT2 (**Fig. 5C**). Circ_0006220 silencing downregulated GOT2 expression, and GOT2

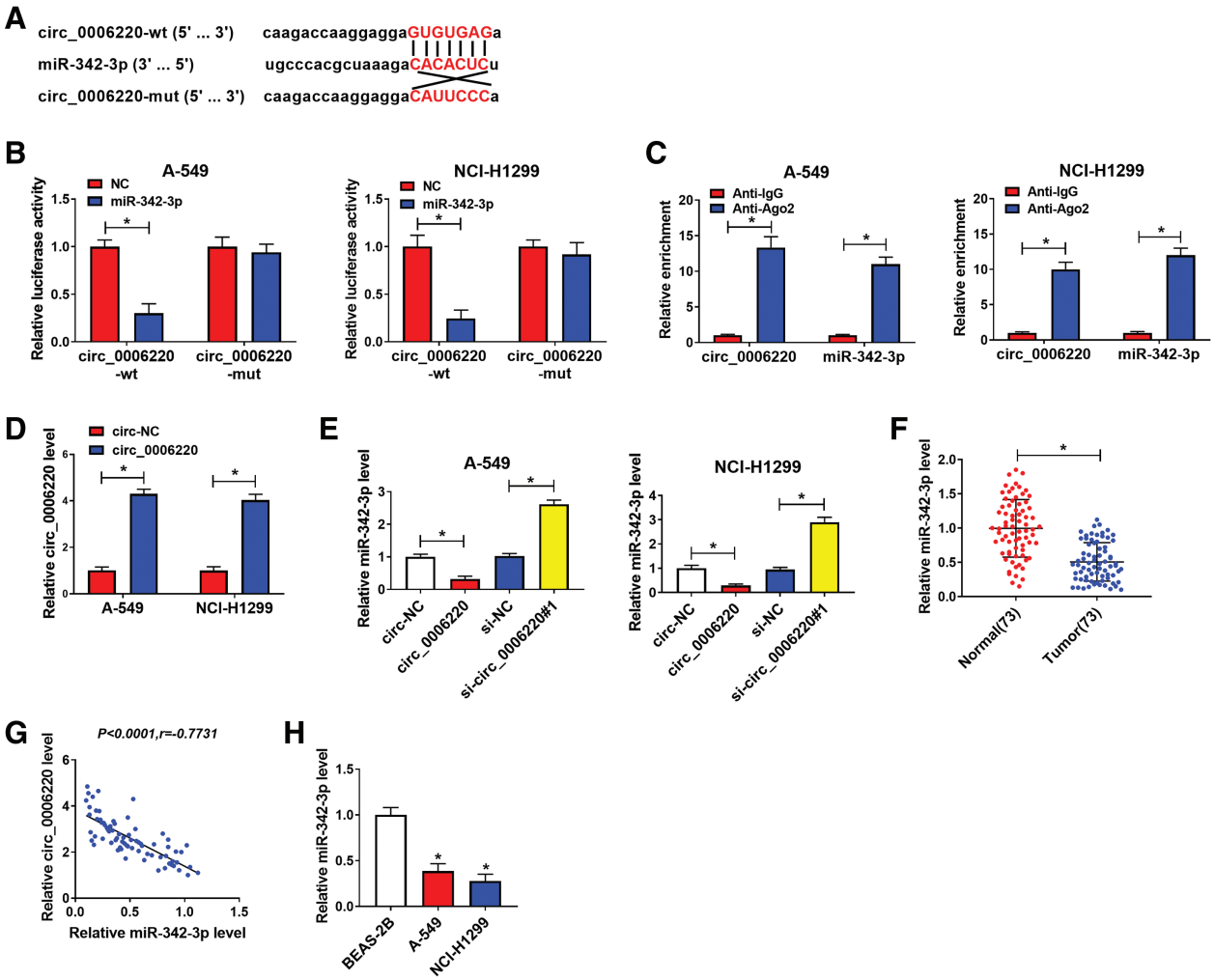

Fig. 3 Circ_0006220 acts as a sponge for miR-342-3p. (**A**) The targets of circ_0006220 were predicted using bioinformatics database StarBase, and miR-342-3p was a candidate target of circ_0006220. (**B**) Dual-luciferase reporter assay was conducted to verify the binding between circ_0006220 and miR-342-3p. With the overexpression of miR-342-3p or not, the luciferase activities of wild-type plasmid (circ_0006220-wt) and mutant-type plasmid (circ_0006220-mut) were determined in NSCLC cells. (**C**) RIP assay was conducted to verify the binding between circ_0006220 and miR-342-3p. (**D**) RT-qPCR was applied to analyze the overexpression efficiency of circ_0006220 plasmid. (**E**) The effect of circ_0006220 overexpression or knockdown on the expression of miR-342-3p was examined by RT-qPCR. (**F**) The level of miR-342-3p was determined in NSCLC specimens (n = 73) and matched normal specimens (n = 73) by RT-qPCR. (**G**) Linear correlation between the expression of circ_0006220 and miR-342-3p was analyzed. (**H**) RT-qPCR was adopted to measure the expression of miR-342-3p in BEAS-2B cells and NSCLC cells. **P* <0.05. NSCLC: non-small cell lung cancer; RIP: RNA immunoprecipitation; RT-qPCR: reverse transcription-quantitative polymerase chain reaction; NC: negative control; IgG: immunoglobulin G; Ago2: Argonaute2; si-NC: negative control siRNA

expression was largely rescued by miR-342-3p silencing (**Fig. 5D**), demonstrating that circ_0006220 positively regulated GOT2 expression by sponging miR-342-3p in NSCLC cells. GOT2 mRNA and protein expression were both upregulated in NSCLC tissues compared with adjacent normal tissues (**Figs. 5E** and **5F**). A positive correlation between the expression of circ_0006220 and GOT2 mRNA was found (**Fig. 5G**), and there was a negative correlation between the expression of GOT2 mRNA and miR-342-3p (**Fig. 5H**). GOT2 protein level was upregulated in A-549 and NCI-H1299 cells relative to BEAS-2B cells (**Fig. 5I**). Overall, GOT2 was a target of miR-342-3p and was regulated by circ_0006220/miR-342-3p axis. In addition, the xenograft experiments manifested that circ_0006220 silencing restrained tumor growth *in vivo* via miR-342-3p/GOT2 axis (**Supplementary Fig. 2**).

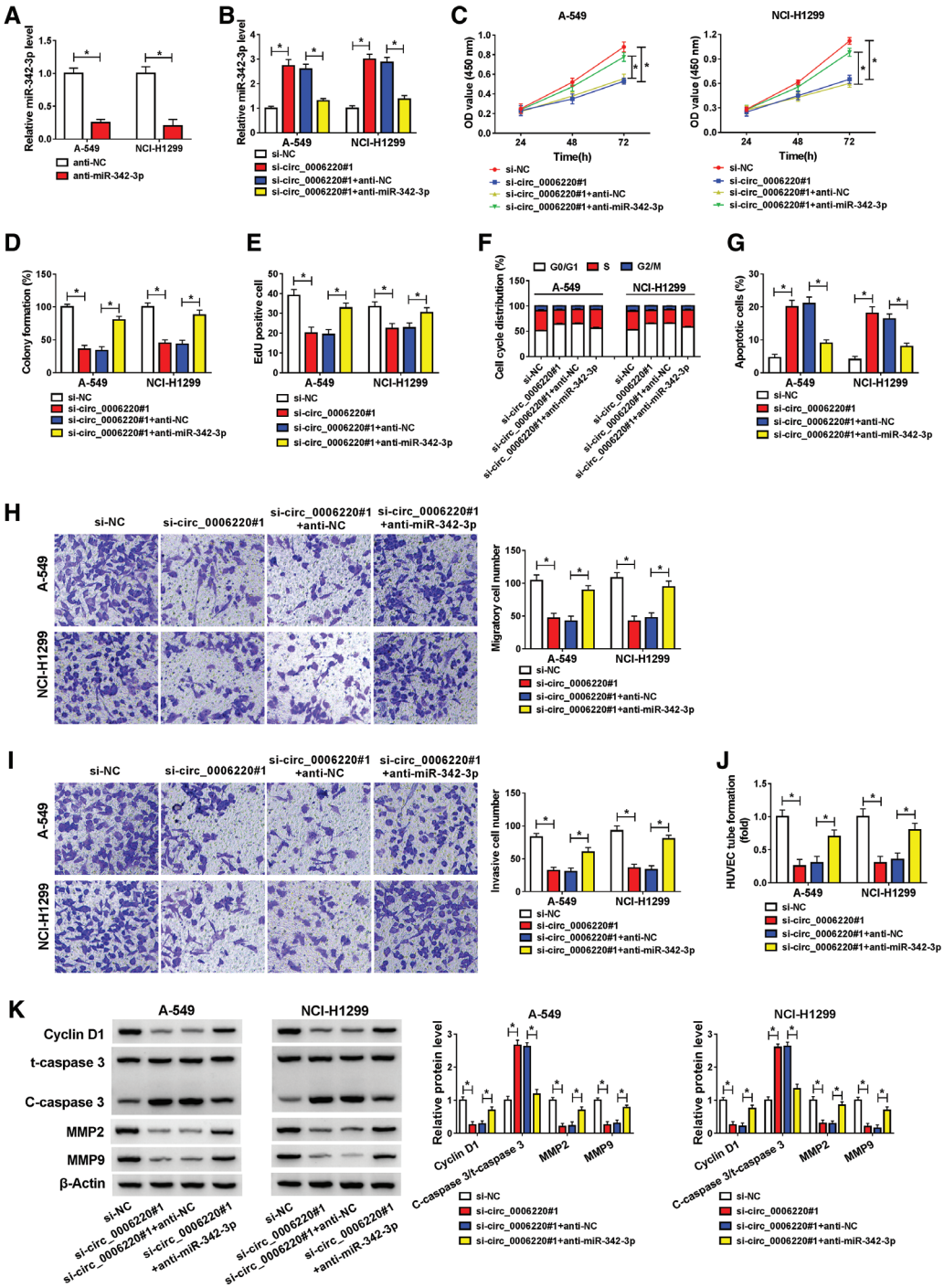

Fig. 4 Circ_0006220 plays an oncogenic role partly by sponging miR-342-3p in NSCLC cells. (**A**) RT-qPCR was adopted to assess the silence efficiency of anti-miR-342-3p in NSCLC cells. (**B**–**K**) NSCLC cells were transfected with si-circ_0006220#1 or si-circ_0006220#1 + anti-miR-342-3p along with their matched controls. (**B**) The level of miR-342-3p was determined by RT-qPCR. (**C**) CCK8 assay was performed to estimate the number of NSCLC cells in each time point to generate cell proliferation curve. (**D**) Cell proliferation was analyzed by colony formation assay. (**E**) EdU assay was applied to assess DNA synthesis rate to analyze cell proliferation. (**F**) Flow cytometry was used to analyze cell cycle progression. (**G**) Cell apoptosis was assessed by flow cytometry. (**H** and **I**) Cell migration and invasion abilities were analyzed by transwell assays. (**J**) Cell angiogenesis ability was analyzed by capillary-like network formation assay. (**K**) The levels of cell markers related to cell proliferation, apoptosis, and motility were determined by Western blot assay. **P* <0.05. NSCLC: non-small cell lung cancer; RT-qPCR: reverse transcription-quantitative polymerase chain reaction; CCK8: Cell Counting Kit-8; EdU: 5-ethynyl-2'-deoxyuridine; NC: negative control; si-NC: negative control siRNA; HUVEC: human umbilical vein endothelial cell line; MMP2: matrix metallopeptidase 2; MMP9: matrix metallopeptidase 9

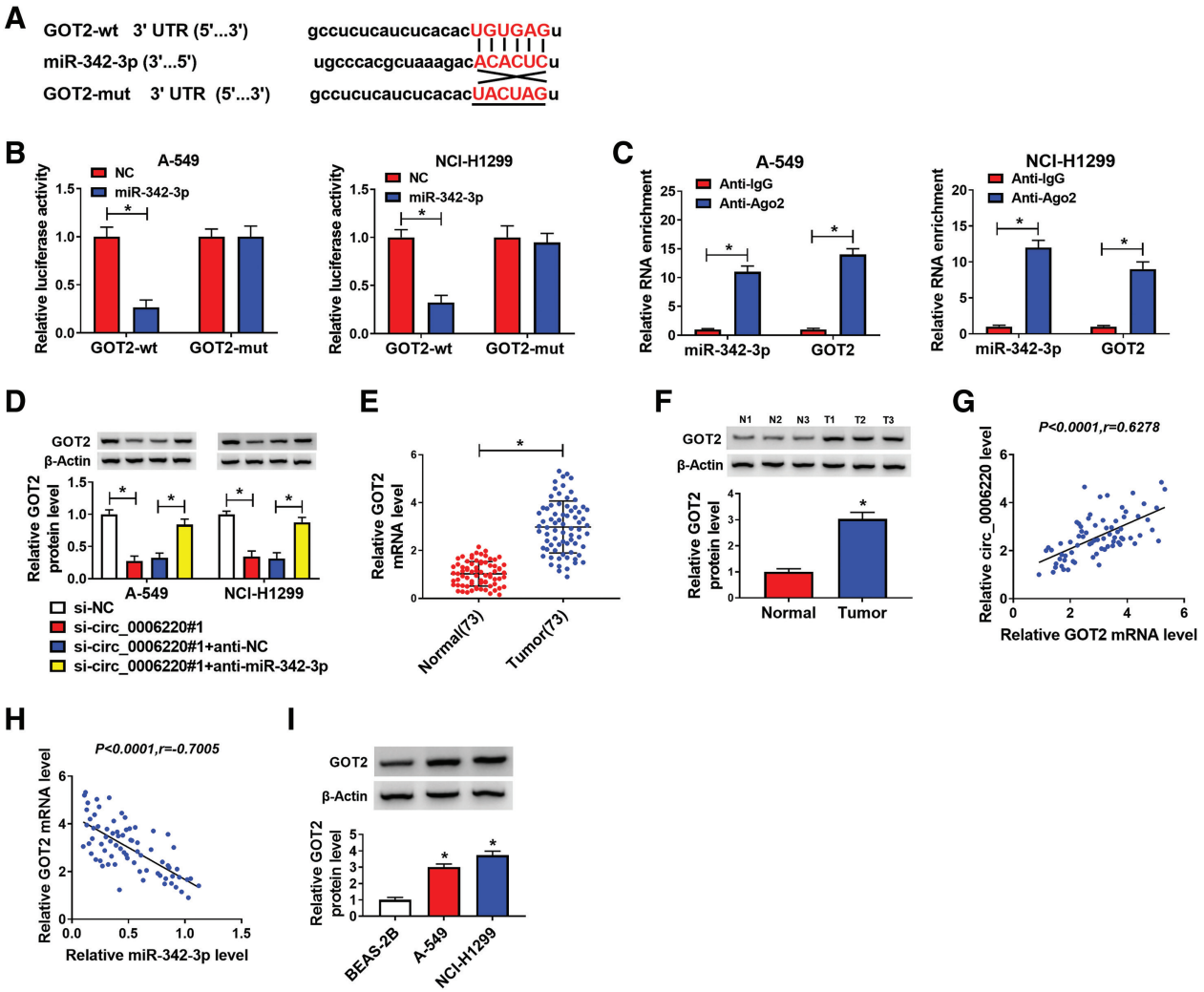

Fig. 5 GOT2 is controlled by circ_0006220/miR-342-3p axis and circ_0006220 exerts its oncogenic roles via miR-342-3p/GOT2 axis. (**A**) StarBase database was used to predict the possible targets of miR-342-3p, and GOT2 was a candidate target of miR-342-3p. (**B** and **C**) Dual-luciferase reporter assay and RIP assay were performed to confirm the binding between miR-343-3p and GOT2. (**D**) NSCLC cells were introduced with si-circ_0006220#1 alone or together with anti-miR-342-3p, and GOT2 protein expression was determined by Western blot assay. (**E** and **F**) The mRNA and protein expression of GOT2 were determined in NSCLC tissues (n = 73) and adjacent normal tissues (n = 73) by RT-qPCR and Western blot assay. (**G** and **H**) Linear correlation between the expression of GOT2 mRNA and circ_0006220 or miR-342-3p was evaluated. (**I**) The protein expression of GOT2 was examined in BEAS-2B and NSCLC cells by Western blot assay. **P* <0.05. GOT2: glutamic-oxaloacetic transaminase 2; RIP: RNA immunoprecipitation; NSCLC: non-small cell lung cancer; RT-qPCR: reverse transcription-quantitative polymerase chain reaction; 3' UTR: 3' untranslated region; NC: negative control; IgG: immunoglobulin G; Ago2: Argonaute2; si-NC: negative control siRNA

Discussion

Currently, circRNAs have shown important regulatory roles in multiple diseases, including vascular diseases,[23,24] heart failure,[25] and cancers.[25] In NSCLC, circRNAs play crucial roles in regulating cell proliferation, motility, apoptosis, and chemo-resistance.[10,14] For example, circ_0067934 knockdown is reported to restrain the proliferation and motility of NSCLC cells, and patients with a high level of circ_0067934 are associated with poor prognosis. Circ_100565 is reported to contribute to the proliferation and motility of NSCLC cells.[26] Chen *et al*. found that circ_0078767 expression is downregulated in NSCLC tissues, and it suppresses the progression of NSCLC by binding to miR-330-3p to induce the expression of Ras association domain family 1 isoform A (RASSF1A).[21] Based on the data of GSE101586,[21] circ_0006220 is reported to be upregulated in NSCLC specimens than that in adjacent normal specimens. Subsequently, we collected 73 pairs of NSCLC tissues and adjacent normal tissues to

confirm the expression feature of circ_0006220. Consistently, we found that circ_0006220 level was elevated in NSCLC specimens relative to matched healthy specimens. Meanwhile, we found that circ_0006220 was notably upregulated in the serum samples of NSCLC patients compared with those of healthy volunteers. The expression pattern of circ_0006220 in different cancers may be different or even opposite. For example, in breast cancer, circ_0006220 is reported to be downregulated in cancer tissues compared with adjacent normal tissues,[22] and the level of circ_0006220 is negatively correlated with aggressive phenotypes of cancer.[27] This phenomenon may be due to the complexity of tumorigenesis and the differences in tumor microenvironment. Compared with BEAS-2B cell line, we found that circ_0006220 level was upregulated in A-549 and NCI-H1299 cell lines. Patients with high expression of circ_0006220 were associated with short survival time. Through loss-of-function experiments, we found that circ_0006220 knockdown suppressed the proliferation, migration, invasion, and angiogenesis but induced the apoptosis of NSCLC cells.

CircRNAs can regulate the biological phenotypes of cancer cells by acting as miRNA sponges.[28] We found that circ_0006220 was majorly distributed in the cytoplasmic fraction of NSCLC cells, indicating that it might function as an miRNA sponge. miR-342-3p was a possible target of circ_0006220 through bioinformatics analysis using the StarBase database. Accumulating evidence demonstrated that miR-342-3p blocks the development of various malignancies. For instance, miR-342-3p is reported to suppress the motility of ovarian cancer cells by reducing the Forkhead Box Q1 level. miR-342-3p is reported to restrain the aggressive phenotypes of nasopharyngeal cancer cells.[29] miR-342-3p is reported to inhibit the growth of hepatocellular carcinoma by suppressing IGF-1R-induced glycolytic metabolism.[30] In NSCLC, miR-342-3p is reported to hamper the malignant phenotypes of cancer cells by targeting multiple downstream molecules, including LASP1,[13] RAP2B, or AGR2. In this study, miR-342-3p was verified to be a target of circ_0006220. We found that miR-342-3p expression was decreased in NSCLC. Moreover, circ_0006220 silencing-induced suppressive effects on the malignant behaviors of NSCLC cells were largely attenuated by the knockdown of miR-342-3p, manifesting that circ_0006220 silencing suppressed NSCLC progression largely by upregulating miR-342-3p.

miRNAs bind to target mRNAs to induce the degradation or suppress the translation of mRNAs. The interaction between miR-342-3p and GOT2 was validated in this study. Aspartate is an important molecule in cell cycle progression, and GOT2 is an aspartate aminotransferase. Previous articles reported that GOT2 regulates cancer cell metabolism in multiple aspects. A previous study pointed out the pro-tumor role of GOT2 in NSCLC in promoting the proliferation, motility, and malate-aspartate metabolism of NSCLC cells.[19] We found that the GOT2 level was elevated in NSCLC tissue specimens and cell lines. miR-342-3p overexpression restrained the malignant behaviors of NSCLC cells, and cell malignant potential was largely rescued by the addition of GOT2 overexpression plasmid, manifesting that miR-342-3p inhibited NSCLC development largely by downregulating GOT2. Circ_0006220 positively regulated GOT2 expression by serving as miR-342-3p sponge in NSCLC cells.

The xenograft mice model was used to analyze the role of circ_0006220 on tumor growth *in vivo*. Circ_0006220 knockdown suppressed tumor growth *in vivo*. In addition, circ_0006220 silencing reduced the expression of proliferation-related molecules in resected tumor tissues.

In future, the *in vivo* role of circ_0006220 in modulating the metastasis of NSCLC tumors needs to be explored. Also, the clinical correlation between circ_0006220 abundance and clinicopathologic features in NSCLC patients needs to be investigated.

Conclusion

In conclusion, this study demonstrated that circ_0006220 facilitated the proliferation, migration, invasion, and tube formation abilities, and suppressed the apoptosis of NSCLC cells by targeting the miR-342-3p/GOT2 axis. The circ_0006220/miR-342-3p/GOT2 axis is a novel potential therapeutic target for NSCLC therapy.

Ethics Approval and Consent to Participate

The present study was approved by the ethical review committee of Wuxi Huishan District People's Hospital. Written informed consent was obtained from all enrolled patients.

Consent for Publication

Patients agreed to participate in this work.

Availability of Data and Materials

The analyzed data sets generated during the present study are available from the corresponding author on reasonable request.

Disclosure Statement

The authors declare that they have no competing interests.

References

1) Siegel RL, Miller KD, Jemal A. Cancer statistics, 2020. CA Cancer J Clin 2020; **70**: 7–30.
2) Herbst RS, Morgensztern D, Boshoff C. The biology and management of non-small cell lung cancer. Nature 2018; **553**: 446–54.
3) Mao Y, Yang D, He J, et al. Epidemiology of lung cancer. Surg Oncol Clin N Am 2016; **25**: 439–45.
4) Duma N, Santana-Davila R, Molina JR. Non-small cell lung cancer: epidemiology, screening, diagnosis, and treatment. Mayo Clin Proc 2019; **94**: 1623–40.
5) Kristensen LS, Andersen MS, Stagsted LVW, et al. The biogenesis, biology and characterization of circular RNAs. Nat Rev Genet 2019; **20**: 675–91.
6) Chen LL, Yang L. Regulation of circRNA biogenesis. RNA Biol 2015; **12**: 381–8.
7) Kulcheski FR, Christoff AP, Margis R. Circular RNAs are miRNA sponges and can be used as a new class of biomarker. J Biotechnol 2016; **238**: 42–51.
8) Qi X, Zhang DH, Wu N, et al. ceRNA in cancer: possible functions and clinical implications. J Med Genet 2015; **52**: 710–8.
9) Zhang HD, Jiang LH, Sun DW, et al. CircRNA: a novel type of biomarker for cancer. Breast Cancer 2018; **25**: 1–7.
10) Kristensen LS, Hansen TB, Venø MT, et al. Circular RNAs in cancer: opportunities and challenges in the field. Oncogene 2018; **37**: 555–65.
11) Yao LX, Liu J, Xu L. MiR-610 functions as a tumor suppressor in oral squamous cell carcinoma by directly targeting AGK. Eur Rev Med Pharmacol Sci 2019; **23**: 187–97.
12) Sun H, Chen Y, Fang YY, et al. Circ_0000376 enhances the proliferation, metastasis, and chemoresistance of NSCLC cells via repressing miR-384. Cancer Biomark 2020; **29**: 463–73.
13) Shen Q, Sun Y, Xu S. LINC01503/miR-342-3p facilitates malignancy in non-small-cell lung cancer cells via regulating LASP1. Respir Res 2020; **21**: 235.
14) Xie X, Liu H, Wang M, et al. miR-342-3p targets RAP2B to suppress proliferation and invasion of non-small cell lung cancer cells. Tumour Biol 2015; **36**: 5031–8.
15) Xue X, Fei X, Hou W, et al. miR-342-3p suppresses cell proliferation and migration by targeting AGR2 in non-small cell lung cancer. Cancer Lett 2018; **412**: 170–8.
16) Hsu PP, Sabatini DM. Cancer cell metabolism: Warburg and beyond. Cell 2008; **134**: 703–7.
17) Vander Heiden MG, Cantley LC, Thompson CB. Understanding the Warburg effect: the metabolic requirements of cell proliferation. Science 2009; **324**: 1029–33.
18) DeBerardinis RJ, Mancuso A, Daikhin E, et al. Beyond aerobic glycolysis: transformed cells can engage in glutamine metabolism that exceeds the requirement for protein and nucleotide synthesis. Proc Natl Acad Sci USA 2007; **104**: 19345–50.
19) Jin M, Shi C, Hua Q, et al. High circ-SEC31A expression predicts unfavorable prognoses in non-small cell lung cancer by regulating the miR-520a-5p/GOT-2 axis. Aging (Albany NY) 2020; **12**: 10381–97.
20) Livak KJ, Schmittgen TD. Analysis of relative gene expression data using real-time quantitative PCR and the 2(-Delta Delta C(T)) method. Methods 2001; **25**: 402–8.
21) Chen T, Yang Z, Liu C, et al. Circ_0078767 suppresses non-small-cell lung cancer by protecting RASSF1A expression via sponging miR-330-3p. Cell Prolif 2019; **52**: e12548.
22) Liang ZZ, Guo C, Zou MM, et al. circRNA-miRNA-mRNA regulatory network in human lung cancer: an update. Cancer Cell Int 2020; **20**: 173.
23) Cao Q, Guo Z, Du S, et al. Circular RNAs in the pathogenesis of atherosclerosis. Life Sci 2020; **255**: 117837.
24) Fasolo F, Di Gregoli K, Maegdefessel L, et al. Non-coding RNAs in cardiovascular cell biology and atherosclerosis. Cardiovasc Res 2019; **115**: 1732–56.
25) Devaux Y, Creemers EE, Boon RA, et al. Circular RNAs in heart failure. Eur J Heart Fail 2017; **19**: 701–9.
26) Li L, Wei H, Zhang H, et al. Circ_100565 promotes proliferation, migration and invasion in non-small cell lung cancer through upregulating HMGA2 via sponging miR-506-3p. Cancer Cell Int 2020; **20**: 160.
27) Liu C, Chen M, Shi Y. Downregulation of hsa_circ_0006220 and its correlation with clinicopathological factors in human breast cancer. Gland Surg 2021; **10**: 816–25.
28) Hansen TB, Jensen TI, Clausen BH, et al. Natural RNA circles function as efficient microRNA sponges. Nature 2013; **495**: 384–8.
29) Cui Z, Zhao Y. microRNA-342-3p targets FOXQ1 to suppress the aggressive phenotype of nasopharyngeal carcinoma cells. BMC Cancer 2019; **19**: 104.
30) Liu W, Kang L, Han J, et al. miR-342-3p suppresses hepatocellular carcinoma proliferation through inhibition of IGF-1R-mediated Warburg effect. Onco Targets Ther 2018; **11**: 1643–53.